

# EVOLUTION OF 3 - 9 $M_{\odot}$ STARS FOR $Z = 0.001 - 0.03$ AND METALLICITY EFFECTS ON TYPE IA SUPERNOVAE

HIDEYUKI UMEDA, KEN'ICHI NOMOTO

Research Center for the Early Universe, and  
 Department of Astronomy, School of Science, University of Tokyo,  
 Bunkyo-ku, Tokyo 113-0033, Japan  
 E-mail: umeda@iron.astron.s.u-tokyo.ac.jp; nomoto@astron.s.u-tokyo.ac.jp

HITOSHI YAMAOKA,

Department of Physics, Faculty of Science, Kyushu University,  
 Ropponmatsu, Fukuoka 810-8560, Japan  
 E-mail: yamaoka@rc.kyushu-u.ac.jp

SHINYA WANAJO

Division of Theoretical Astrophysics  
 National Astronomical Observatory, Mitaka, Tokyo 181-8588, Japan  
 E-mail: wanajo@diamond.mtk.nao.ac.jp

## ABSTRACT

Recent observations have revealed that Type Ia supernovae (SNe Ia) are not perfect standard candles but show some variations in their absolute magnitudes, light curve shapes, and spectra. The C/O ratio in the SNe Ia progenitors (C-O white dwarfs) may be related to this variation. In this work, we systematically investigate the effects of stellar mass ( $M$ ) and metallicity ( $Z$ ) on the C/O ratio and its distribution in the C-O white dwarfs by calculating stellar evolution from the main-sequence through the end of the second dredge-up for  $M = 3 - 9M_{\odot}$  and  $Z = 0.001 - 0.03$ . We find that the total carbon mass fraction just before SN Ia explosion varies in the range  $0.36 - 0.5$ . We also calculate the metallicity dependence of the main-sequence-mass range of the SN Ia progenitor white dwarfs. Our results show that the maximum main-sequence mass to form C-O white dwarfs decreases significantly toward lower metallicity, and the number of SN Ia progenitors may be underestimated if metallicity effect is neglected. We discuss the implications of these results on the variation of SNe Ia, determination of cosmological parameters, luminosity function of white dwarfs, and the galactic chemical evolution.

*Subject headings:* stars: evolution — stars: interiors — stars: white dwarfs — stars: supernovae:  
 general — stars: abundances — nuclear reactions

## 1. INTRODUCTION

Type Ia supernovae (SNe Ia) are characterized by the absence of hydrogen and the presence of strong Si II line in the early time spectra. Majority of SNe Ia have almost the same absolute brightness, thereby being good distance indicators for determining cosmological parameters (e.g., Branch and Tammann 1992; Sandage and Tammann 1993; Nomoto, Iwamoto, & Kishimoto 1997 for a recent review). However, SNe Ia are not perfect standard candles but show some variations in their absolute magnitudes, light curve shapes, and spectra (Phillips 1993; Branch, Romanishin, & Baron 1996; Hamuy et al. 1996). It is important to understand the source of these variations and the dependence on the metallicity in order to use high-redshift SNe Ia for determining the cosmological parameters.

It is widely accepted that SNe Ia are thermonuclear explosions of accreting C-O white dwarfs (WDs), although detailed explosion mechanism is still under debate (e.g. Ruiz-Lapuente, Canal, & Isern 1997). Previous studies have shown that typical SNe Ia are well described by the Chandrasekhar mass model, in which accreting C-O WDs explode when the masses of these WDs approach the critical mass  $M_{\text{Ia}} \simeq 1.37 - 1.38M_{\odot}$  (Nomoto, Thielemann, & Yokoi 1984; Höflich & Khokhlov 1996). The explosion is induced by the carbon ignition in the central region and the subsequent propagation of the burning front. Be-

hind the burning front, explosive burning produces a large amount of  $^{56}\text{Ni}$ . There are two models for the burning front propagation: the deflagration model (e.g., Ivanova et al. 1974; Nomoto, Sugimoto, & Neo 1976; Nomoto et al. 1984) and the delayed (or late) detonation (DD) model (Khokhlov 1991; Yamaoka et al. 1992; Woosley & Weaver 1994).

There are several possible sources of the variations of brightness and spectra: for example, variations of the age of the WDs and the mass accretion rates, which affect the ignition density, variations of the WD progenitor's main-sequence mass and metallicity, which affect the C/O ratio in the WDs, and the variation of the deflagration-detonation transition density ( $\rho_{tr}$ ) in the DD model. These effects modify the explosion energy and the synthesized  $^{56}\text{Ni}$  mass, which affects the maximum brightness and shape of the SN Ia light curve.

Regarding the C/O ratio, previous explosion models have been constructed by assuming a uniform mass fraction ratio  $C/O = 1$ , though previous results indicated  $C/O < 1$  in the central region (e.g. Mazzitelli, & D'Antona 1986 a,b; Schaller et al. 1992, SSMM hereafter). This is partly for simplicity and partly due to its strong sensitivity on the treatment of convection and the  $^{12}\text{C}(\alpha, \gamma)^{16}\text{O}$  rate. However, the effect of the different C/O ratio is not negligible. For example, recently Höflich, Wheeler, &

Thielemann (1998) constructed explosion models by arbitrarily changing the C/O ratio to  $C/O = 2/3$  and found some significant effects on the light curve and spectra.

Intermediate mass stars by definition burn only hydrogen and helium, and form C-O cores after He burning. These cores will become C-O WDs, thus becoming SNe Ia progenitors in certain binary systems. Previously, several groups have investigated intermediate mass stars, but they have not paid much attention to the C/O ratio and the C-O core mass size with its systematic dependence on the stellar mass and metallicity, as well as its effects on SNe Ia. For example, SSMM and a series of subsequent papers (Schaerer et al. 1993; Charbonnel et al. 1993) studied the influence of the metallicity on the life times, luminosities and the chemical structure. However, they only showed the central and surface chemical abundances and did not show the C-O core mass sizes. Salaris et al. (1997) showed the radial profile of the C/O ratio in the intermediate mass stars as well as the C-O core mass size, but only for solar metallicity. Vassiliadis & Wood (1993) calculated C-O core mass sizes for the stars below  $5 M_{\odot}$ , but did not pay much attention to the C/O ratio. The works prior to 1992, such as Castellani et al. (1990), Tornambé & Chieffi (1986), Becker & Iben (1979), used Los Alamos (Huebner et al. 1977) or Cox & Stewart (1970) opacity tables, and hence their results would be significantly different if latest OPAL opacity (Iglesias & Rogers 1993) was used.

In this paper, using updated input physics, we evolve the intermediate mass ( $3 - 9 M_{\odot}$ ) stars and examine the stellar metallicity and mass dependence of the C/O ratio, its radial profile, and the C-O core mass size. These quantities are sensitive to the treatment of convective mixing; however, for the same treatment of convection, the  $^{12}\text{C}(\alpha, \gamma)^{16}\text{O}$  rate dominantly determines these. As described in section 2, we calibrate this rate by the massive star nucleosynthesis.

We also obtain metallicity dependence of zero-age main-sequence (ZAMS) mass ranges of SN Ia progenitors, and especially its upper limit  $M_{\text{UP}}$ , where  $M_{\text{UP}}$  is the ZAMS mass at the border between the star that ignites carbon under non-degenerate condition and the star that forms a strong degenerate C-O core. This quantity is important for various applications, such as galactic chemical evolution and the luminosity function of WDs in our galaxy. However, earlier determination of  $M_{\text{UP}}$  was based on old radiative opacity tables (e.g. Becker & Iben 1979, BI79 hereafter; Castellani et al. 1985, CCPT hereafter; Tornambé & Chieffi 1986; Castellani et al. 1990) or not by exact calculations (Schaerer et al. 1993). Also the calculations during the 1980s and early 1990s often assumed strong overshooting or breathing pulses, which may not be preferable with the use of the OPAL opacity. Their results are qualitatively consistent with our results but quantitatively different. Our  $M_{\text{UP}}$  is significantly smaller than the estimates in BI79 for all  $Z$  we calculated, and in Schaerer et al. (1993) for  $Z \lesssim 0.01$ , and it shows a large decrease toward lower metallicity. Such a dependence would be important for the distributions of SNe Ia brightness as a function of metallicity.

This paper is organized as follows. In the next section, our numerical code, input physics and parameters are de-

scribed. Section 3 shows our results and compares with previous works. Their implications are discussed in Section 4.

## 2. NUMERICAL CODE AND ASSUMPTIONS

We modify and update the Henyey type stellar evolution code (Saio & Nomoto 1988). Important improvements include the use of the OPAL radiative opacity (Iglesias & Rogers 1993), neutrino emissivity (Itoh, Nishikawa, & Kohyama 1996) and a nuclear reaction network with larger number of isotopes. Most of the nuclear reaction rates are provided by Thielemann (1995). This network is coupled to the dynamical equations for stellar evolution *implicitly* in a similar manner as SSMM and Weaver & Woosley (1993). That is, the network with a reduced number of isotopes is run during Henyey relaxation. Nuclear energy generation rates between the reduced and full networks are almost identical. After dynamics is converged, nucleosynthesis is calculated with a full network code for He burning. The isotopes included are shown in Table 1. For H burning, the network code of Saio & Nomoto (1988) is used with updated nuclear reaction rates.

Treatment of convection is one of the serious uncertainties in the theory of stellar evolution. We adopt the Schwarzschild criterion for convective instability and the diffusive treatment for the convective mixing (Spruit 1992; Saio & Nomoto 1998). This formalism contains a parameter  $f_k$  of order unity which is proportional to the diffusion coefficient, and also to the square root of the ratio of “soluble” to thermal diffusivity. We found that the results were not sensitive to this parameter at least in the range  $f_k \simeq 0.1 - 1$ . In this paper, we set  $f_k = 0.3$ . We use the mixing length parameter  $\alpha = 1.5$  for the outermost super-adiabatic convection. Chieffi, Straniero, & Salaris (1995) found that a larger value ( $\alpha \simeq 2.25$ ) fits observations well with the use of OPAL opacity. However, as shown in the next section, in our code the evolutionary tracks in the H-R diagram are closer to those of SSMM for  $\alpha = 1.5$ . Also as described in the next section, the core property, especially the central C/O ratio, is insensitive to this parameter. Therefore, our conclusions in this paper are little affected by the choice of a different  $\alpha$ . We neither artificially enhance nor suppress convective regions from the Schwarzschild criterion throughout the calculations, and hence we do not include convective overshooting and breathing pulses at the end of He burning. It is considered that with the use of the OPAL opacity these effects are not so large as considered before (e.g. Stothers & Chin 1991); however, whether these effects are significant or not is still uncertain.

Once the treatment of convection is fixed, the  $^{12}\text{C}(\alpha, \gamma)^{16}\text{O}$  rate dominantly determines the C/O ratio after He burning and the C-O core mass size. Since the track in the H-R diagram is not sensitive to the  $^{12}\text{C}(\alpha, \gamma)^{16}\text{O}$  rate, it is very difficult to constrain this rate from the surface property of the stars, such as spectral observations of clusters. In this paper this rate is chosen to be 1.5 times the value of Caughlan & Fowler (1988, CF88 hereafter). This choice, denoted by  $1.5 \times \text{CF88}$ , with the same treatment for the convection yields the central carbon mass fraction  $X(^{12}\text{C}) \simeq 0.20$  after the He burning of the  $25 M_{\odot}$  star (Umeda & Nomoto 1998). Therefore, it approxi-

mately reproduces the central C/O ratio of the Nomoto & Hashimoto (1988, NH88 hereafter) model, being expected to be consistent with solar abundances of Ne/O and Mg/O in massive star yield (Hashimoto, Nomoto, & Shigeyama 1989; Thielemann, Nomoto, & Hashimoto 1996; Woosley & Weaver 1995). We note that although the  $^{12}\text{C}(\alpha, \gamma)^{16}\text{O}$  rate is constrained most stringently by the nucleosynthesis argument of massive star yield (Weaver & Woosley 1993; Thielemann et al. 1996), our knowledge of this rate is still limited, because there are still uncertainties in the chemical evolution, massive star evolution, and the explosive nuclear burning models. In Section 3.3, we examine the dependence of this rate by applying the rates of 1.7, 1.5, and 1.0 times the rate of CF88 and the rate of Caughlan et al. (1985, CF85 hereafter). More detailed investigation of the C/O ratio in massive stars, and its dependence on  $^{12}\text{C}(\alpha, \gamma)^{16}\text{O}$  rate and treatments of convection will be given in Umeda & Nomoto (1998).

We adopt the solar chemical composition by Anders & Grevesse (1989), the solar He abundance  $Y_{\odot}=0.27753$  and metallicity  $Z_{\odot}=0.02$  (Bahcall & Pinsonneault 1995). We assume that the initial (zero age main sequence or ZAMS) helium abundance depends on metallicity  $Z$  as  $Y(Z) = Y_p + (\Delta Y/\Delta Z)Z$  (for  $Z \leq 0.02$ ), where  $\Delta Y/\Delta Z$  is a constant and  $Y_p$  is the primordial helium abundance. In this paper we adopt  $Y_p = 0.247$  (Tytler, Fan, & Burles 1996), and thus  $\Delta Y/\Delta Z = 1.5265$ . For  $Z > 0.02$ , we only show the case of  $(Z, Y)=(0.03, 0.28)$ . Different  $Y$  yields different stellar evolution. Especially, the star is brighter for a larger  $Y$ . However, as shown below the effects of changing  $Y$  is not very large.

We also include an empirical mass loss rate (de Jager, Nieuwenhuijzen, & van der Hucht 1988) being scaled with metallicity as  $(Z/0.02)^{0.5}$  (Kudritzki et al. 1989).

### 3. RESULTS

We calculated the evolution of intermediate-mass ( $3 - 9 M_{\odot}$ ) stars for metallicity  $Z=0.001 - 0.03$ . Figure 1 shows the evolution in the H-R diagram and the central density ( $\rho_c$ ) vs. central temperature ( $T_c$ ) diagram of our  $5 M_{\odot}$  ( $Z=0.02$ ) model compared with SSMM. The luminosity of our model tends to be lower than SSMM and  $\rho_c$  is higher for the same  $T_c$ . There are many differences in the inputs, which may be the reasons for these differences: we adopt  $Y = 0.2775$  for  $Z = 0.02$ , while SSMM assumed  $Y = 0.3$ . Our choice of the  $^{12}\text{C}(\alpha, \gamma)^{16}\text{O}$  rate ( $1.5 \times \text{CF88}$ ) are smaller than  $\text{CF85} \sim 2.3 \times \text{CF88}$  in SSMM. We use the larger nuclear reaction network. The treatment of convection is different. Especially they assumed overshooting from a convective core, which we do not. Figure 1 shows that the difference of  $Y$  alone does not explain the discrepancy. Also, we find that the tracks on the H-R diagrams are almost identical even though the  $^{12}\text{C}(\alpha, \gamma)^{16}\text{O}$  rate is different. Therefore, probably the treatment of convection is mainly responsible for the differences. Indeed, the tracks on the H-R diagrams of the no-overshooting models in Bressan et al. (1993) are similar to our results.

In this figure we also show the effect of mixing length parameter  $\alpha$  for the outermost super-adiabatic convection. This parameter changes the location in the H-R diagram after a star becomes a red giant. On the other hand, the central  $\rho_c - T_c$  track is almost independent of this param-

eter. As a result, the central C/O ratio is almost identical between the  $\alpha = 1.5$  and  $2.25$  cases. Therefore, the choice of this parameter is not so important for the purpose of this paper. Chieffi et al. (1995) found that  $\alpha = 2.25$  fits observations well; however, the evolutionary tracks in the H-R diagram are closer to those of SSMM for  $\alpha = 1.5$  than  $2.25$ , and hence we adopt  $\alpha = 1.5$  in the followings.

#### 3.1. Metallicity effects on stellar evolution

In the ranges of stellar masses and  $Z$  considered in this paper, the most important metallicity effect is that the radiative opacity is smaller for lower  $Z$ . Therefore, a star with lower  $Z$  is brighter, thus having a shorter lifetime than a star with the same mass but higher  $Z$ . In this sense, the effect of reducing metallicity for these stars is almost equivalent to increasing a stellar mass. This is verified in Figure 2, which shows the H-R diagrams of the  $5 M_{\odot}$  models for different metallicities (upper panel) and the models with  $Z = 0.02$  for different stellar masses (lower panel).

For stars with larger masses and/or smaller  $Z$ , the luminosity is higher at the same evolutionary phase. With a higher nuclear energy generation rate, these stars have larger convective cores during H and He burning, thus forming larger He and C-O cores. This property is depicted in Figure 3(a) and (b).

Figure 3(a) shows abundances in mass fraction in the inner core of the  $7 M_{\odot}$  star for  $Z=0.001$  at age  $t=48.45$  Myr, with the central temperature and density  $\log T_c$  (K)=8.58 and  $\log \rho_c$  ( $\text{g cm}^{-3}$ )=6.82. In Figure 3(a), the He burning shell is located around the mass coordinate  $M_r = 1.1 M_{\odot}$ , which indicates that the C-O core of this model will exceed  $1.1 M_{\odot}$ . Since this is well above the critical mass for the off-center carbon ignition, this star will ignite carbon in the non-degenerate region and will not form a C-O WD but form an O-Ne-Mg core (Nomoto 1984).

If the star is less massive or has higher metal abundance than the model in Figure 3(a), the C-O core can be smaller and the carbon ignition is avoided as shown in Figure 3(b) for the  $7 M_{\odot}$  model of  $Z=0.02$  at age  $t=51.87$  Myr (at the end of the second dredge-up). The dredge-up is a phenomenon during which the surface convection is penetrating inwards and the inner material is being brought up to the surface. The first dredge-up occurs before or around the He ignition and the second one occurs during the He shell burning stage for intermediate-mass stars. During the second dredge-up phase, the thick He shell which is seen in Figure 3(a) becomes thinner and thinner because of the C-O core growth through He shell burning and the penetration of the surface convection. Therefore, as shown in Figure 3(b), the He shell becomes very thin (in mass coordinate) at the end of the second dredge-up phase. Chemical abundances at the end of the second dredge-up for the 6 and  $4 M_{\odot}$  stars (with  $Z = 0.02$ ) are also shown in Figures 4 and 5, respectively.

#### 3.2. ZAMS mass ranges of SN Ia progenitors

The stars that do not ignite carbon will evolve into the asymptotic giant branch (AGB) phase. During this phase, if they are single stars, the C-O core mass increases slightly due to H-He double shell burning until they lose almost all hydrogen-rich envelopes by wind mass loss. If they

are in close binary systems, their hydrogen-rich envelopes will be stripped off in much shorter time scale due to the Roche lobe overflow, and C-O WDs are left. When the companion star evolves off the main-sequence, mass transfer occurs from the companion star to the WD. A certain class of these accreting WDs become SNe Ia depending on the accretion rate and the initial mass of the WD (e.g., Nomoto 1982; Nomoto & Kondo 1991).

The WD mass at the onset of mass transfer from the companion star (denoted by  $M_{\text{WD},0}$ ) is critically important for the fate of the accreting WD. For  $M_{\text{WD},0}$  as low as  $\lesssim 0.7M_{\odot}$ , the WD mass is difficult to reach  $M_{\text{Ia}} \simeq 1.37 - 1.38M_{\odot}$ . For higher  $M_{\text{WD},0}$ , the WD can become SNe Ia in a certain binary system (Hachisu, Kato, & Nomoto 1996; Li & van den Heuvel 1996). However, the  $M_{\text{WD},0}$  depends on various uncertain factors, such as a binary separation, effects of recurring He shell flashes, and a mass loss rate during the AGB phase. In the following discussion, we assume that  $M_{\text{WD},0}$  is not significantly larger than the C-O core mass at the end of the second dredge-up phase, which we denote  $M_{\text{CO}}$ .

Figure 6 shows the metallicity dependence of the relation between the ZAMS mass ( $M_{\text{ms}}$ ) and  $M_{\text{CO}}$ . We note that stars with higher metallicity form smaller C-O cores if they have the same  $M_{\text{ms}}$ . Our  $M_{\text{ms}}$  vs.  $M_{\text{CO}}$  relations are similar to Castellani et al. (1990) which used Los Alamos Opacity (Huebner et al. 1977) and assumed overshooting but suppressed breathing pulses at the end of He burning. They calculated  $Z=0.02, 0.006, 0.002$  and  $Y=0.23, 0.27$  cases for 3, 4, 5, 7, 9  $M_{\odot}$  stars. Our  $M_{\text{ms}}$  vs.  $M_{\text{CO}}$  relations are also consistent with Vassiliadis & Wood (1993), which used OPAL opacity without overshooting.

Figure 7 shows  $M_{\text{UP}}$  as a function of metallicity, which is compared with BI79 and CCPT. Our results in these figures are quantitatively different from BI79, because BI79 used old Cox & Stewart (1970) opacity. Our results are also different from CCPT's because they assumed relatively large overshooting. Although Castellani et al. (1990) did not estimate  $M_{\text{UP}}$  exactly, their results indicate that their  $M_{\text{UP}}$  lies closer to ours than those of BI79 and CCPT. CCPT and Castellani et al. (1990) assumed strong overshooting, but we note that when OPAL opacity is used the overshooting effect should not be very large to meet the observational constraints (Stothers & Chin 1991). Schaerer et al. (1993) also estimated  $M_{\text{UP}}$  by comparing their grids of stellar models with  $T_c$  vs.  $\rho_c$  tracks in Maeder & Meynet (1989), which is shown in Figure 7 by the crosses. Our results show a stronger metallicity dependence than Schaerer et al. (1993). Especially, their  $M_{\text{UP}}$  at  $Z=0.001$  is significantly larger than ours.

Tornambé & Chieffi (1986) studied  $M_{\text{UP}}$  for very extremely metal-deficient stars ( $Z \leq 10^{-4}$ ) and found that the  $M_{\text{UP}}$  increases for smaller  $Z$ . Though verifying this result may be interesting, we do not treat these extremely low metal stars because stars with  $Z < 10^{-3}$  may not become SNe Ia progenitors in the Chandrasekhar mass model (Kobayashi et al. 1998).

In Figure 7, we also plot  $M_{\text{LO}}$ , which is defined to be the lower ZAMS mass limit for stars to become SNe Ia. Here we assume that in order for the accreting WD to reach  $M_{\text{Ia}}$ ,  $M_{\text{CO}}$  should be larger than a certain critical mass, typically  $\sim 0.8M_{\odot}$  (Hachisu et al. 1996). Since this crit-

ical  $M_{\text{CO}}$  depends on the binary parameters, three cases of  $M_{\text{CO}}$  are shown in Figure 7.

In Figure 8 we show the number of SNe Ia progenitors, i.e. the number of stars in the range  $M_{\text{LO}} \leq M \leq M_{\text{UP}}$ , normalized to the case of  $Z = 0.02$  and  $M_{\text{CO}} = 0.8M_{\odot}$ . Since  $M_{\text{LO}}$  is sensitive to the binary parameters, we consider four cases of  $M_{\text{LO}}$  in Figure 8. In obtaining this figure, Salpeter IMF is used. This figure shows that if Salpeter IMF holds also in a lower metallicity environment, the number of SNe Ia progenitors increase toward low metallicity, because stars with lower metallicity have larger C-O cores for the same  $M_{\text{ms}}$ . It should be noted that these numbers do not necessarily proportional to the SNe Ia rate, because we need to take into account the binary companion's lifetime in order to calculate the SNe Ia rate.

### 3.3. C/O ratio in white dwarfs

From Figures 3-5, we find that the central part of these stars is oxygen-rich. The C/O ratio is nearly constant in the innermost region, which was a convective core during He burning. Outside this homogeneous region, where the C-O layer grows due to He shell burning, the C/O ratio increases up to  $\text{C/O} \gtrsim 1$ ; thus the oxygen-rich core is surrounded by a shell with  $\text{C/O} \gtrsim 1$ . In fact this is a generic feature in all models we calculated. The C/O ratio in the shell is  $\text{C/O} \simeq 1$  for the star as massive as  $\sim 7M_{\odot}$  (Fig. 3b), and  $\text{C/O} > 1$  for less massive stars (Figs. 4 and 5).

In most cases of our calculations as well as previous ones, from the center to the C-O core edge the oxygen abundance has a peak near the outer edge of the oxygen-rich core. This configuration is Rayleigh-Taylor unstable and will be rehomogenized by convection (Salaris et al. 1997; Isern et al. 1998). Their results show that the rehomogenization proceeds slowly and the effect is relatively small during the liquid phase of the WD interior. However, because of this effect the final chemical profile of the inner SNe Ia progenitors may differ from the profile at the end of second dredge-up depending on the time scale of becoming SNe Ia.

Figure 9 shows the central C/O ratio in mass fraction, which is not a monotonic function of the metallicity and the ZAMS mass. One reason for this complexity is that the C/O ratio is sensitive to the evolutionary change in the convective core size during the later stage of He burning. Small differences in the core temperature and opacity lead to a different evolutionary behavior of the convective core, which largely changes the C/O ratio.

The central C/O ratio is sensitive to the  $^{12}\text{C}(\alpha, \gamma)^{16}\text{O}$  rate. For example, for  $M = 5M_{\odot}$ ,  $Z = 0.02$ , and  $Y = 0.27753$ , this ratio is 0.58 for CF88 $\times 1.5$  rate, while  $\text{C/O} = 0.89, 0.47$ , and  $0.24$  for CF88, CF88 $\times 1.7$ , and CF85 rates, respectively. This ratio, on the other hand, is not so sensitive to  $Y$ : for example,  $\text{C/O}=0.58$  and  $0.53$  for  $Y=0.285$  and  $Y=0.30$ , respectively. Several groups including Salaris et al. (1997) and Bressan et al. (1993) calculated the central C & O mass fractions for solar metallicity. SSMM and a series of subsequent papers calculated the fractions for various metallicities. Our results of the central C/O ratio is systematically larger than those of SSMM and Salaris et al., who adopted the CF85  $^{12}\text{C}(\alpha, \gamma)^{16}\text{O}$  rate and different treatments of convection.

Figure 10 shows the total mass of  $^{12}\text{C}$  ( $M(^{12}\text{C})$ ) integrated over the WD mass,  $M_{\text{Ia}} \simeq 1.37M_{\odot}$ , just before the SN Ia explosion. Here we assume  $\text{C/O} \sim 1$  in the outer layer of  $M_{\text{CO}} \leq M_r \leq M_{\text{Ia}}$  which is formed by He shell burning during accretion. This is because our results as well as other previous works indicate that a star with C-O core mass heavier than  $\sim 1M_{\odot}$  tends to yield  $\text{C/O} \sim 1$  in the product of He shell burning. We note that C/O depends on both the  $(\rho, T)$  track and the nuclear reaction rate. For example, if we use CF88 for the  $^{12}\text{C}(\alpha, \gamma)^{16}\text{O}$  rate in the model of Figure 3(b), the C/O ratio in the shell is  $\text{C/O} \simeq 1.46$ .

The total carbon mass is important for studying SNe Ia, because it determines the total explosion energy. The total carbon mass fraction,  $M(^{12}\text{C})/M_{\text{Ia}}$ , varies in the range of  $0.36 - 0.5$  depending on the ZAMS mass and metallicity, which might be related to the observed variation of the SNe Ia brightness.

In Figures 11 and 12, we plot the central C/O ratio and  $M(^{12}\text{C})$  again, but abscissa is changed to  $M_{\text{CO}}$ . These figures show that by replacing the abscissa from  $M_{\text{ms}}$  to  $M_{\text{CO}}$ , these curves somewhat converge. Its implication is discussed in the next section.

#### 4. SUMMARY AND DISCUSSIONS

We have calculated the stellar evolution through the carbon ignition or the second dredge-up for  $M = 3 - 9M_{\odot}$  and  $Z = 0.001 - 0.03$ . Using these evolutionary models, we have made systematic investigations on the stellar metallicity and mass dependencies of the C-O core mass  $M_{\text{CO}}$  at the end of the second dredge-up, the C/O ratio in the C-O core, and the mass range ( $M_{\text{LO}}, M_{\text{UP}}$ ). The major effect of changing metallicity appears in the  $M_{\text{CO}} - M_{\text{ms}}$  relation (Figs. 9 and 11). Main conclusions and the implication on SNe Ia are as follows:

- 1) The  $Z$  dependence of  $M_{\text{UP}}$  and  $M_{\text{LO}}$  are important to obtain the white dwarf luminosity function, and to model the galactic chemical evolution, because these determines the SNe Ia rate. Our results exhibit that  $M_{\text{UP}}$  and  $M_{\text{LO}}$  are both smaller for lower  $Z$ . This implies that if the initial mass function is independent of metallicity, the number density of SN Ia progenitors are larger in a lower metallicity environment (Fig. 8); therefore, the luminosity function of WDs and SNe Ia would depend on  $Z$ .
- 2) Our results indicate that the innermost part of C-O WDs is likely to be oxygen-rich ( $\text{C/O} \lesssim 0.6$ ) rather than  $\text{C/O} = 1$  as usually assumed in the SNe Ia modeling. We find two tendencies of the central C/O ratio: (1) For a fixed  $Z$ , as stellar mass increases, the C/O ratio at the stellar center first increases to the maximum and then decreases. The location of peaks, which depend on metallicity, are seen at lower mass in our results ( $M_{\text{ms}} \sim 5M_{\odot}$ ) than in SSMM ( $M_{\text{ms}} \sim 7M_{\odot}$ ). (2) For larger  $Z$ , the above maximum C/O ratio is larger. Compared with SSMM, our results show a much larger variation in the C/O ratio distribution.
- 3) For WDs which can be progenitors of SN Ia, the central ratio varies in the range of  $\text{C/O} = 0.4 - 0.6$  depending mainly on the ZAMS mass. The total carbon mass fraction just before SN Ia explosion is found to vary in the range  $M(^{12}\text{C})/M_{\text{Ia}} = 0.36 - 0.5$ . These may be partially responsible for the observed variations in the brightness

and spectra of SNe Ia.

Most of previous works on the SNe Ia explosion have used progenitor models with  $\text{C/O}=1$ . Only recently Höflich et al. (1998) have started calculations with different C/O for the DD models. The variation of C/O ratio would be important, because as the inner regions are burned during the deflagration phase, the energy release is changed and, consequently, the pre-expansion of the outer layers is modified. This changes the total explosion energy, and hence the expansion rate of the SNe Ia, the brightness and shape of light curves as well. Also it may affect the  $\rho_{\text{tr}}$  in the DD model to induce a large variation in the explosion energy.

4) The ranges of the variation in the central C/O ratio and  $M(^{12}\text{C})/M_{\text{Ia}}$  obtained above do not significantly depend on  $Z$  for  $0.001 \leq Z \leq 0.02$ . These ratios shown in Figures 9 and 10 exhibit smaller dispersion with respect to metallicity if these ratios are plotted against  $M_{\text{CO}}$  (Figs. 11 and 12). We conclude that the metallicity effects are relatively minor for the same  $M_{\text{CO}}$ , although there are still some significant variations in the central C/O ratio for  $M_{\text{CO}} \gtrsim 0.8M_{\odot}$  (Fig. 11). Moreover, WDs with  $Z \lesssim 0.002$  need not be considered for SNe Ia progenitors, because such low metallicity WDs blow too weak winds to evolve into SNe Ia (Kobayashi et al. 1998). These would be good for determining cosmological parameters with the use of SNe Ia, because “evolutionary” effects on the SN Ia properties are minor at different red-shifts.

We thank H. Saio for kindly providing us his code, and P. Höflich, N. Prantzos, and F. -K. Thielemann for useful conversation. This work has been supported in part by the grant-in-Aid for Scientific Research (05242102, 06233101, 6728, 10147212) and COE research (07CE2002) of the Ministry of Education, Science and Culture in Japan and by the National Science Foundation in US under Grant No. PHY94-07194.

## REFERENCES

- Anders, E., & Grevesse, N., 1989, *Geochim. Cosmochim. Acta*, 53, 197
- Bahcall, J. N., & Pinsonneault, M. H., 1995, *Rev. of Mod. Phys.*, 67, 781
- Becker, S. A., & Iben, I., 1979, *ApJ*, 232, 831 (BI79)
- Branch, D., Romanishin, W., & Baron, E., 1996, *ApJ*, 465, 73
- Branch, D., & Tammann, G. A., 1992, *ARA&A*, 1992, 30, 359
- Bressan, A., Fagotto, F., Bertelli, G., & Chiosi, C., *A&AS*, 1993, 100, 647
- Castellani, V., Chieffi, A., Pulone, L., & Tornambé, A., 1985, *ApJ*, 294, L31 (CCPT)
- Castellani, V., Chieffi, A., & Straniero, O., 1990, *ApJS*, 74, 463
- Caughlan, G., Fowler, W., Harris, & M. J., Zimmermann, B. A., 1985 *Atomic Data Nucl. Data Tables*, 32, 197 (CF85)
- Caughlan, G., & Fowler, W., 1988, *Atomic Data Nucl. Data Tables*, 40, 283 (CF88)
- Charbonnel, C., Meynet, G., Maeder, A., Schaller, G., & Schaerer, D., 1993, *A&AS*, 101, 415
- Chieffi, A., Straniero, O., & Salaris, M., 1995, *ApJ*, 445, L39
- Cox, A. N. & Stewart, J. N., 1970, *ApJS*, 19, 243
- Hachisu, I., Kato, M., & Nomoto, K., 1996, *ApJ*, 470, L97
- Hamuy, M., Phillips, M. M., Schommer, R. A., & Suntzeff, N. B., 1996, *AJ*, 112, 2391.
- Hashimoto, M., Nomoto, K., & Shigeyama, T., 1989, *A&A*, 210, L5
- Huebner, W. F., Merts, A. L., Magee, N. H., & Argo, M. F., 1977, *Los Alamos Sci. Lab. Rept.*, LA-670-M
- Höfllich, P., & Khokhlov, A., 1996, *ApJ*, 457, 500
- Höfllich, P., Wheeler, J. C., & Thielemann, F. -K., 1998, *ApJ*, 495, 617
- Iglesias, C. A., & Rogers, F. F., 1993, *ApJ*, 412, 752
- Itoh, N., Nishikawa, A., & Kohyama, Y., 1996, *ApJS*, 102, 411
- Ivanova, L. N., Imshennik, V. S., Chechetkin, V. M., 1974, *Ap&SS*, 31, 497
- de Jager, C., Nieuwenhuijzen, H., & van der Hucht, K., 1988, *A&AS*, 72, 259
- Khokhlov, A., 1991, *A&A*, 245, 114; *A&A* 245, L25
- Kobayashi, C., Tsujimoto, T., Nomoto, K., Hachisu, I., & Kato, M., 1998, *ApJ*, 503, L155
- Kudritzki, R., Pauldrach, A., Puls, J., & Abbott, D., 1989, *A&A*, 219, 205
- Li, X.-D., & van den Heuvel, E. P. J., 1997, *A&A*, 322, L9
- Maeder, A., & Meynet, G., 1989, *A&A*, 210, 155
- Mazzitelli, I., & D'Antona, F., 1986a, *ApJ*, 308, 706
- . 1986b, *ApJ*, 311, 762
- Nomoto, K., Sugimoto, D., & Neo, S., 1976, *Ap. Space. Sci.*, 39, L37
- Nomoto, K., 1982, *ApJ*, 253, 798
- Nomoto, K., 1984, *ApJ*, 277, 791
- Nomoto, K., Thielemann, F. -K., & Yokoi, K., 1984, *ApJ*, 286, 644
- Nomoto, K., & Hashimoto, M., 1988, *Phys. Rep.*, 163, 13 (NH88)
- Nomoto, K., & Kondo, Y., 1991, *ApJ*, 367, 119
- Nomoto, K., Iwamoto, K., & Kishimoto, N., 1997, *Science*, 276, 1378
- Phillips, M. M., 1993, *ApJ*, 413, L75
- Ruiz-Lapuente, P., Canal, R., & Isern, J., eds., 1997, "Thermonuclear Supernovae", (Dordrecht, Boston, London: Kluwer)
- Saio, H., & Nomoto, K., 1998, in *Computational Astrophysics: Stellar Physics*, eds. Kudritzki, R., Mihalas, D., Nomoto, K., & Thielemann, F. -K. (New York: Springer), in press
- Salaris, M., Dominguez, I., Garcia-Berro, E., Hernanz, M., Isern, J., & Mochkovitch, R., 1997, *ApJ*, 486, 413
- Sandage, A., & Tammann, G. A., 1993, *ApJ*, 415, 1
- Schaerer, D., Charbonnel, C., Meynet, G., Maeder, A., & Schaller, G., 1993, *A&AS*, 102, 339
- Schaller, G., Schaerer, D., Meynet, G., & Maeder, A., 1992, *A&AS*, 96, 269 (SSMM)
- Spruit, H. C., 1992, *A&A*, 253, 131
- Stothers, R. B., & Chin, C.-W., 1991, *ApJ*, 381, L67
- Thielemann, F. -K., Nomoto, K., & Hashimoto, M., 1996, *ApJ*, 460, 408
- Thielemann, F. -K., 1995, private communication
- Tornambé, A., & Chieffi, A., 1986, *MNRAS*, 220, 529
- Tytler, D., Fan, X.-M., & Burles, S., 1996, *Nature*, 381, 207
- Umeda, H., & Nomoto, K., 1998, in preparation
- Vassiliadis, E., & Wood, P. R., 1993, *ApJ*, 413, 641
- Weaver, T. A., & Woosley, S. E., 1993, *Phys. Rep.*, 227, 665
- Woosley, S. E., & Weaver, T. A., 1994, in *Supernovae, Les Houches Session LIX*, eds. Bludman, S. A., Mochkovitch, R., & Zinn-Justin, J. (Amsterdam: Elsevier), p63
- Woosley, S. E., & Weaver, T. A., 1995, *ApJS*, 101, 181
- Yamaoka, H., Nomoto, K., Shigeyama, T., & Thielemann, F.-K., 1992, *ApJ*, 393, 55

TABLE 1

Isotopes included in the nuclear network for He burning.

Isotope	A	Isotope	A
n	1	H	1
He	4	C	12-13
N	13-15	O	14-18
F	17-19	Ne	18-22
Na	21-23	Mg	22-27
Al	25-29	Si	27-30
Fe	56		

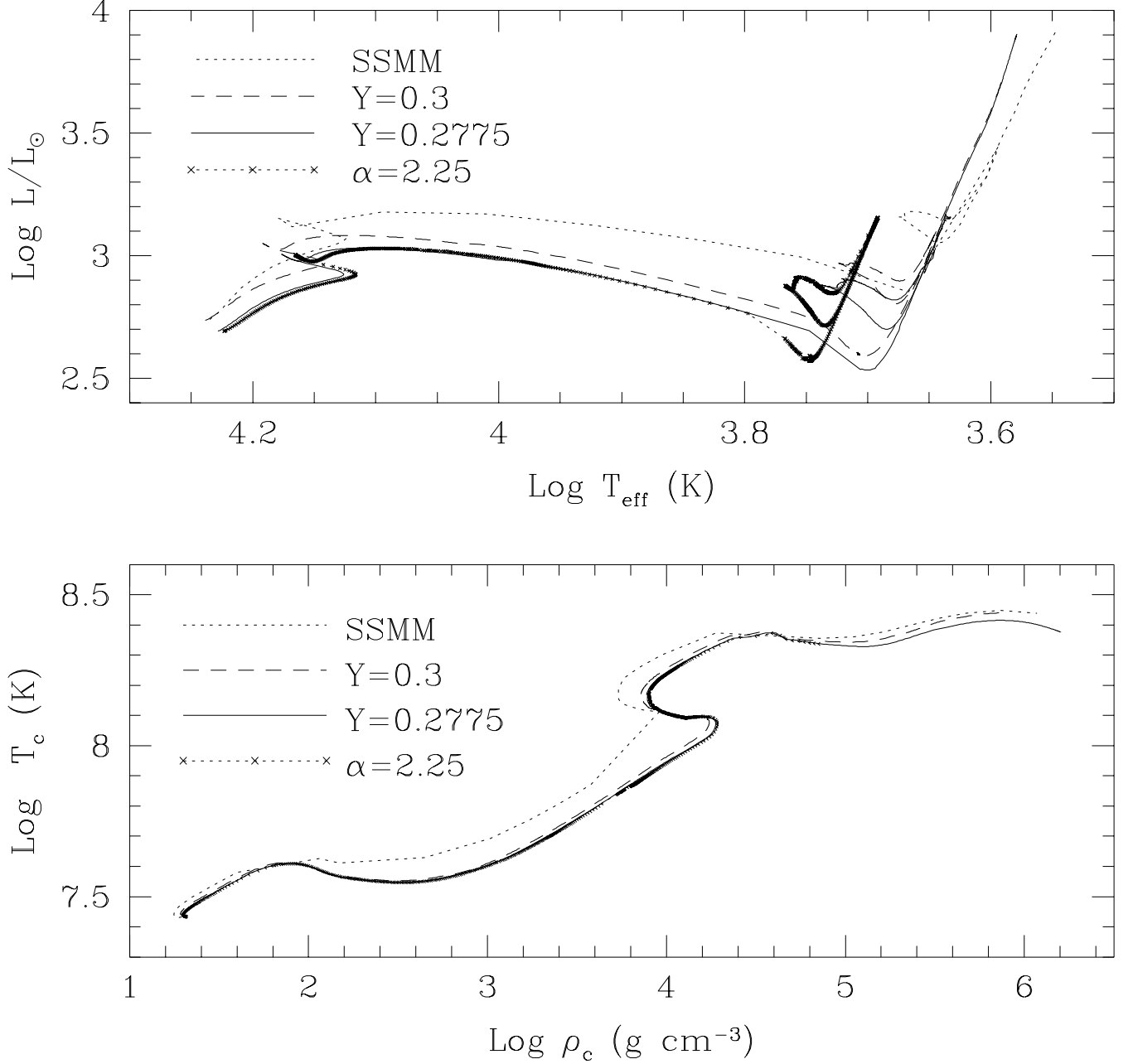


FIG. 1.— Evolution in the H-R diagram (upper panel) and the central density ( $\rho_c$ ) vs. central temperature ( $T_c$ ) diagram (lower panel) of our  $5 M_{\odot}$  ( $Z=0.02$ ) models for  $Y = 0.2775$  (solid), compared with SSMM (dotted; Schaller et al. 1992). Dependence on  $Y$  is small as seen from the case of  $Y = 0.3$  (dashed). A model with a larger mixing length parameter  $\alpha$  ( $=2.25$ ) is shown in a dotted curve with crosses.

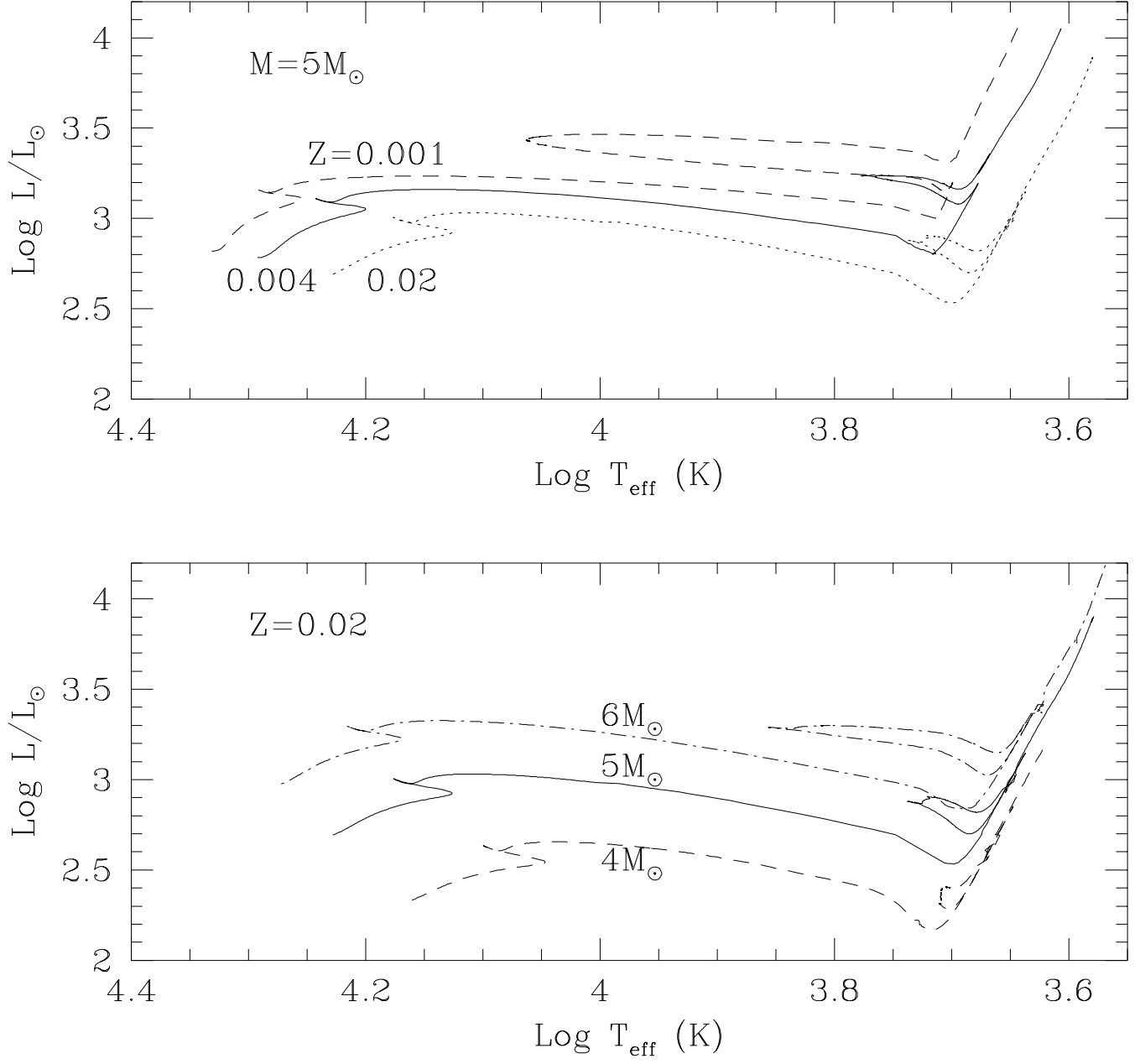


FIG. 2.— Evolution in the H-R diagrams of the  $5M_{\odot}$  models for several metallicities  $Z$  (upper panel) and the  $Z = 0.02$  models for several stellar masses (lower panel).



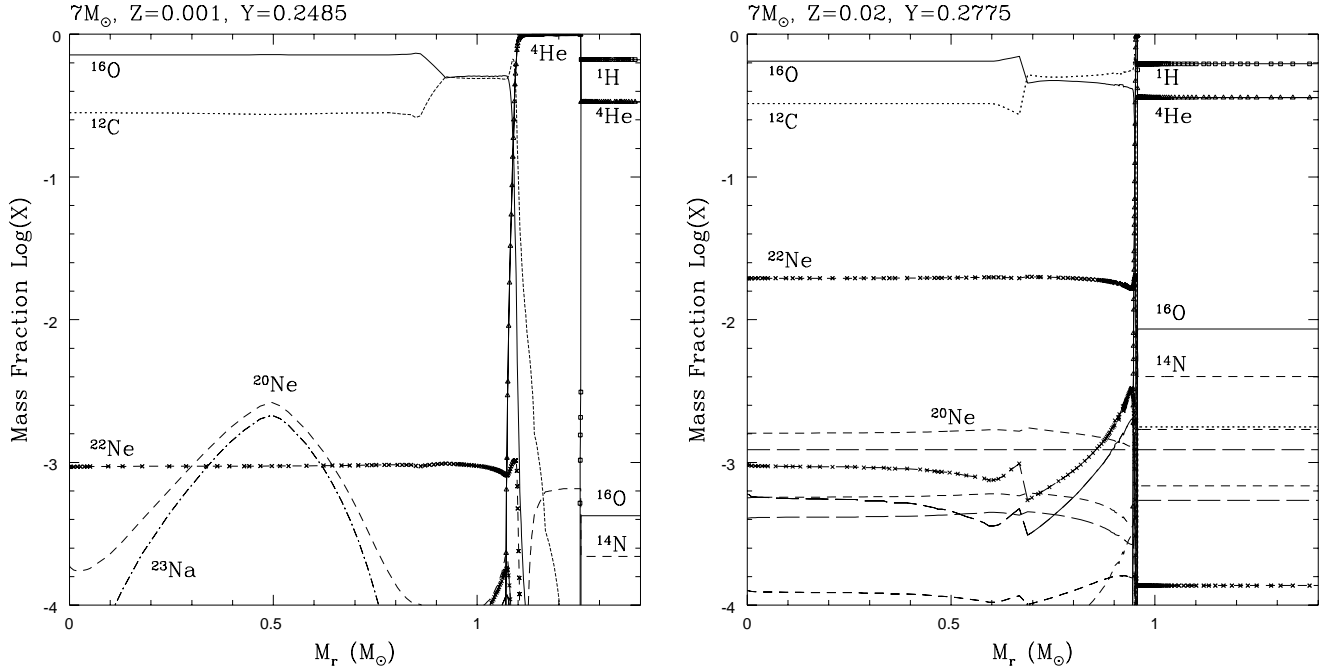


FIG. 3.— (a) Abundances in mass fraction in the inner core of the  $7 M_{\odot}$  star for  $Z=0.001$  at age  $t=48.45$  Myr, with the central temperature and density  $\log T_c$  (K)=8.58 and  $\log \rho_c$  ( $\text{g cm}^{-3}$ ) =6.82 (left panel). The maximum temperature,  $\log T_{\text{max}}=8.78$ , is attained at  $M_r = 0.54 M_{\odot}$ . (b) Same as Figure 3(a) but for  $Z=0.02$  at the end of the second dredge-up,  $t=51.87$  Myr, with  $\log T_c=8.29$  and  $\log \rho_c =7.04$  (right panel). Maximum temperature,  $\log T_{\text{max}}=8.69$ , is attained at  $M_r = 0.72 M_{\odot}$ .

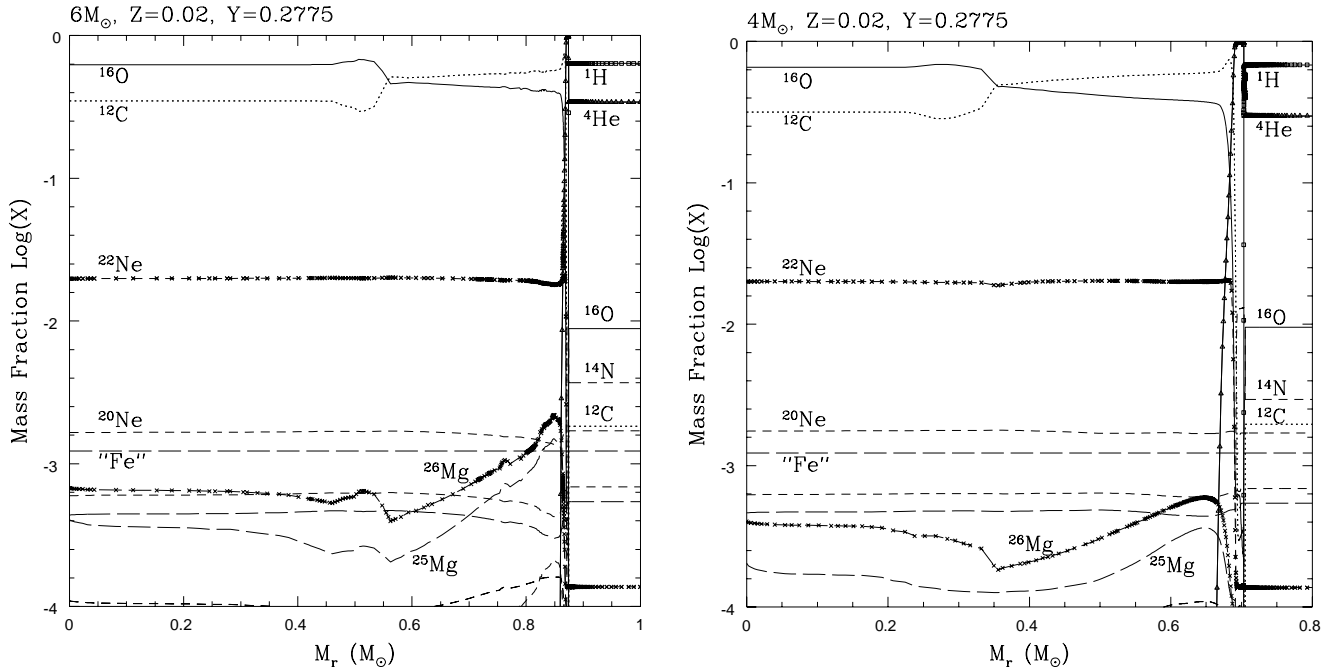


FIG. 4.— Same as Figure 3(b) but for  $M = 6 M_{\odot}$ . (left)

FIG. 5.— Same as Figure 3(b) but for  $M = 4 M_{\odot}$ . (right)

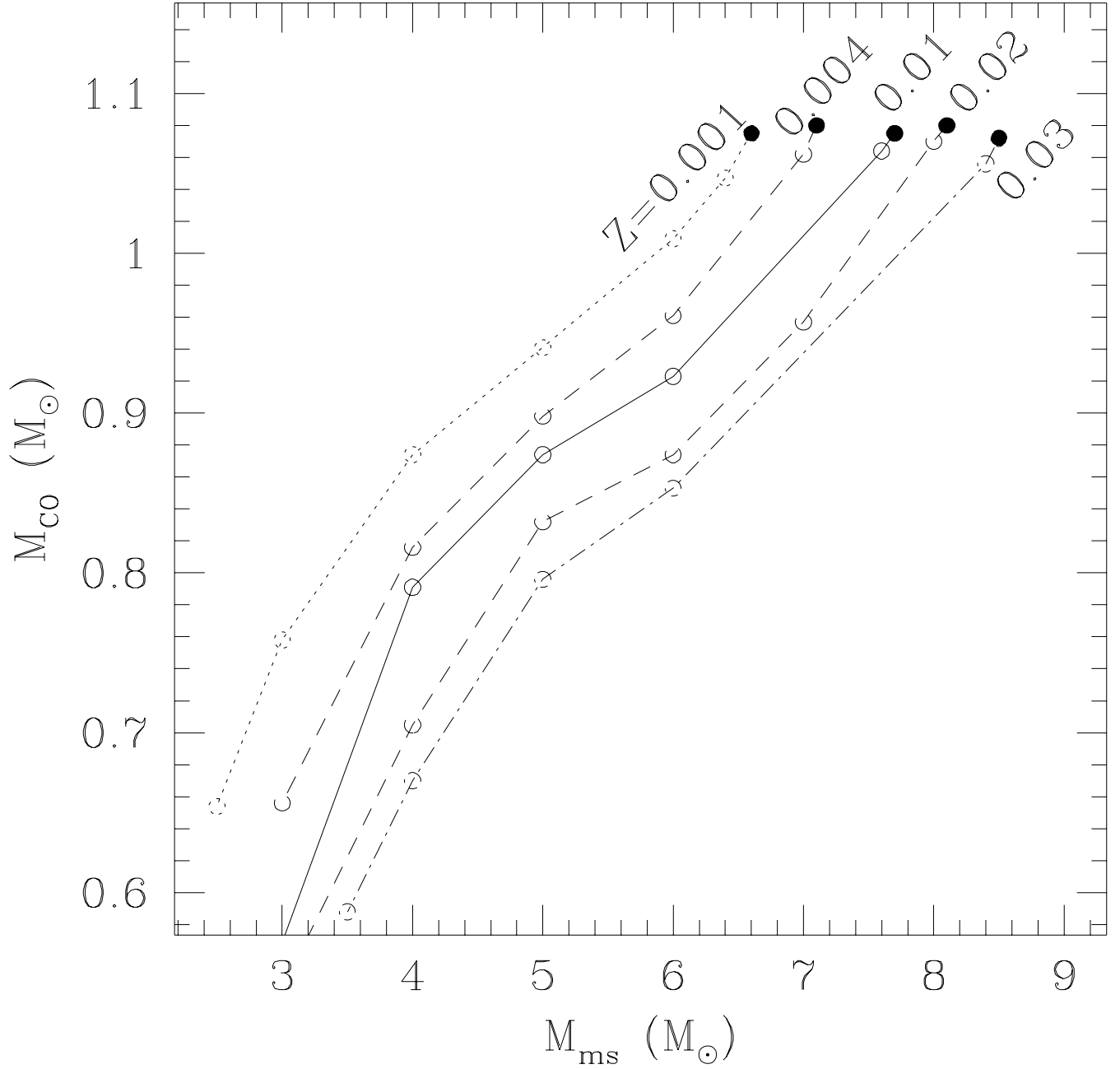


FIG. 6.— Metallicity dependence of the ZAMS mass ( $M_{\text{ms}}$ ) vs. C-O core mass ( $M_{\text{CO}}$ ) at the end of the second dredge-up. Filled circles indicate that off-center carbon ignition occurs in these model. Hence, the abscissa of these points correspond to the  $M_{\text{UP}}$ .

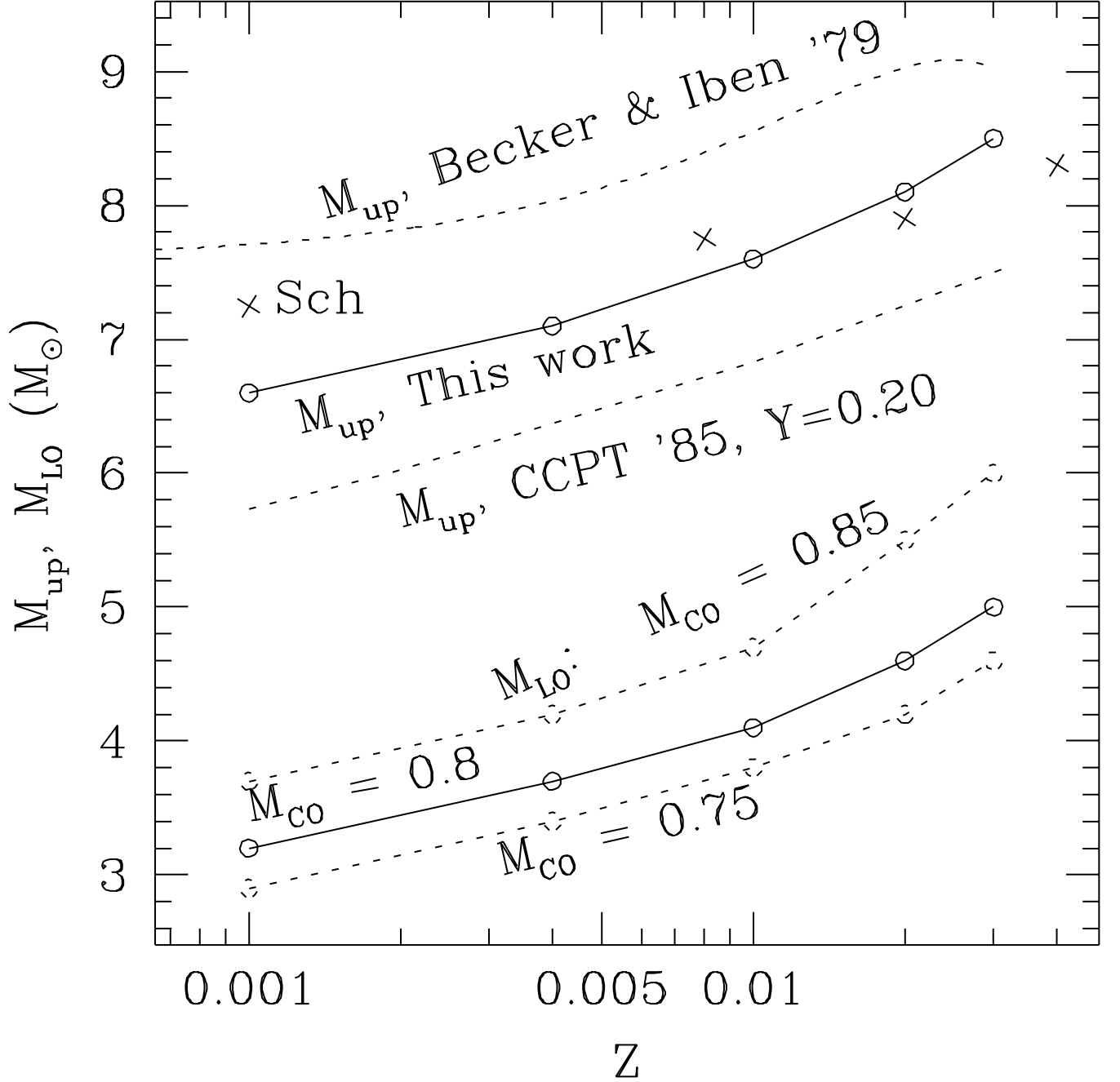


FIG. 7.—  $M_{\text{UP}}$  obtained in this work compared with earlier works. The lower ZAMS mass limit for becoming an SN Ia,  $M_{\text{LO}}$ , is also shown. Since this value depends on the binary parameters, three curves are shown, which correspond to  $M_{\text{CO}} = 0.75, 0.80$  and  $0.85 M_{\odot}$ . Crosses labeled by 'Sch' are  $M_{\text{UP}}$  of Schaerer et al. (1993).

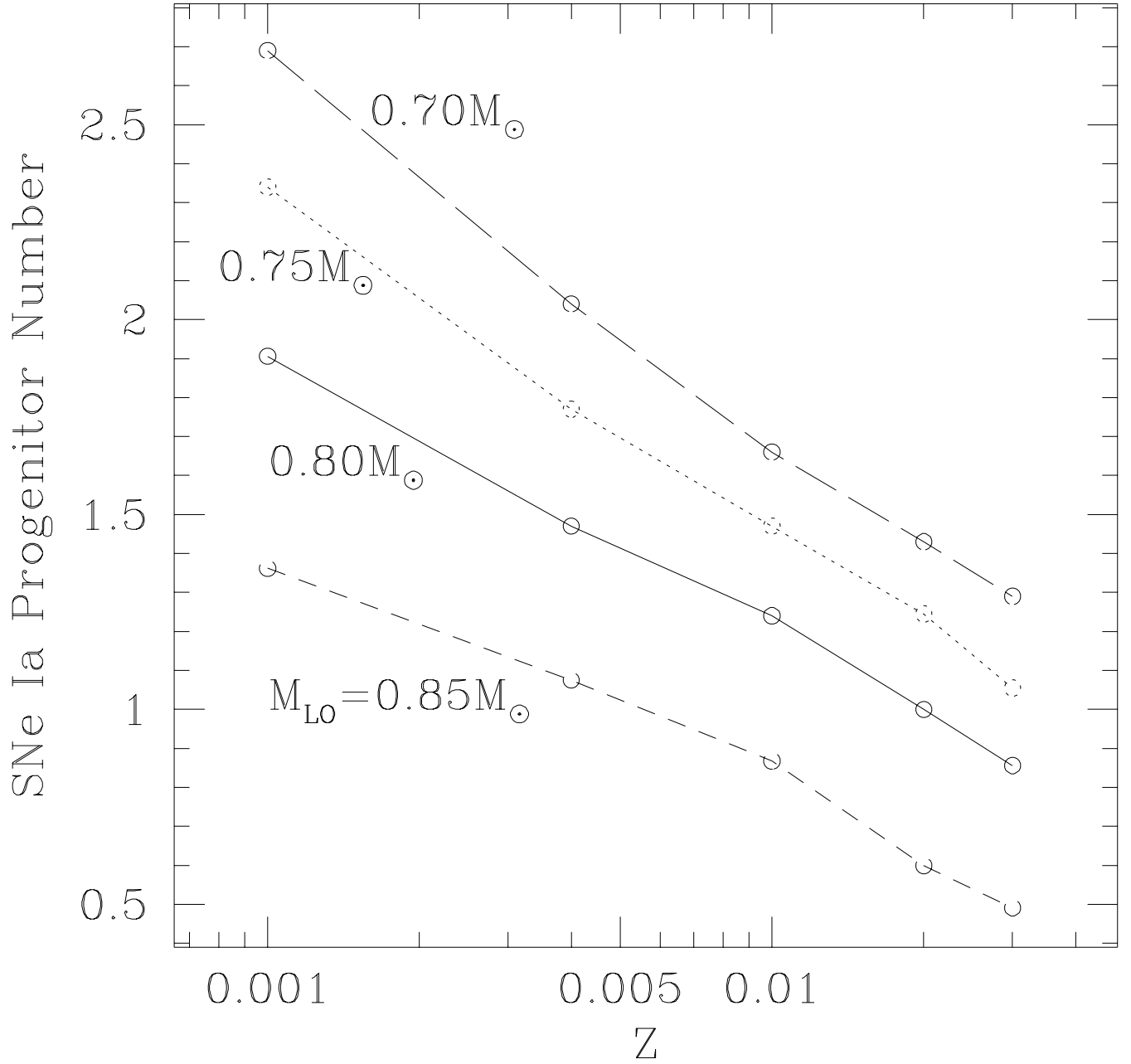


FIG. 8.— Metallicity and  $M_{LO}$  dependence of the number of SNe Ia progenitors normalized to the case with  $Z = 0.02$  and  $M_{LO} = 0.8 M_{\odot}$ . The Salpeter IMF is assumed.

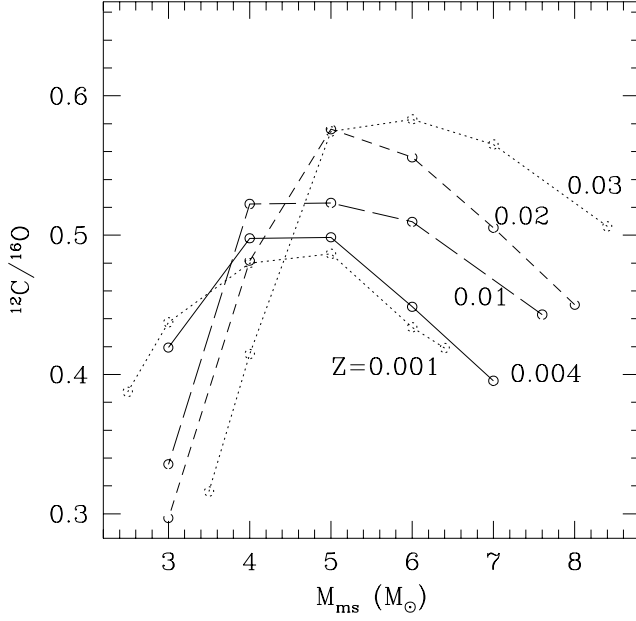


FIG. 9.— Central C/O ratio in mass fraction as a function of metallicity and stellar mass. (left)

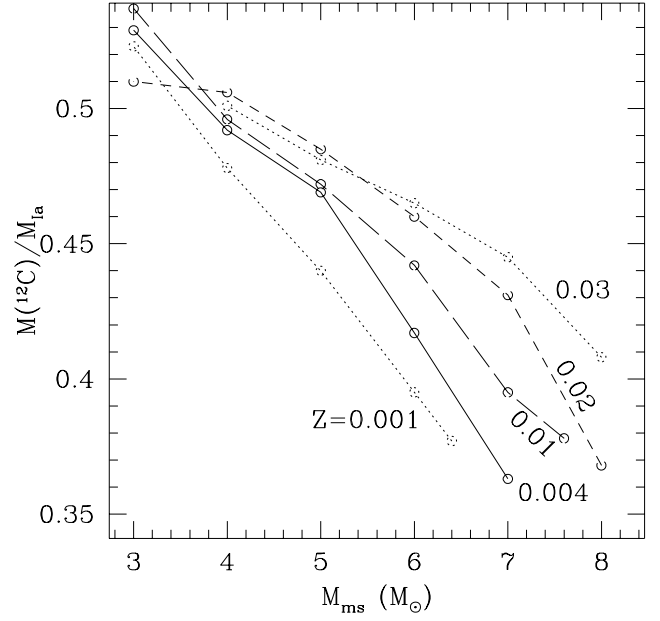


FIG. 10.— Total  $^{12}\text{C}$  mass ( $M(^{12}\text{C})$ ) included in the WD of mass  $M_{\text{Ia}} = 1.37M_{\odot}$  just before an SN Ia explosion as a function of  $M_{\text{ms}}$ . (right)

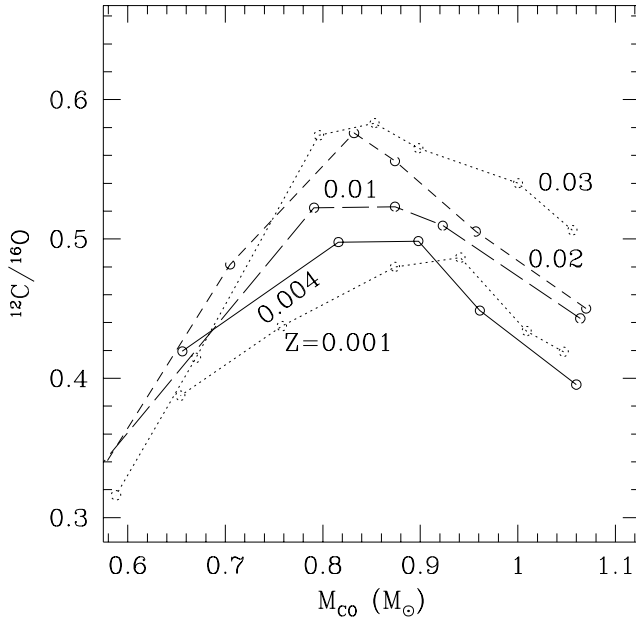


FIG. 11.— Central C/O ratio in mass fraction as a function of metallicity and  $M_{\text{CO}}$ . (left)

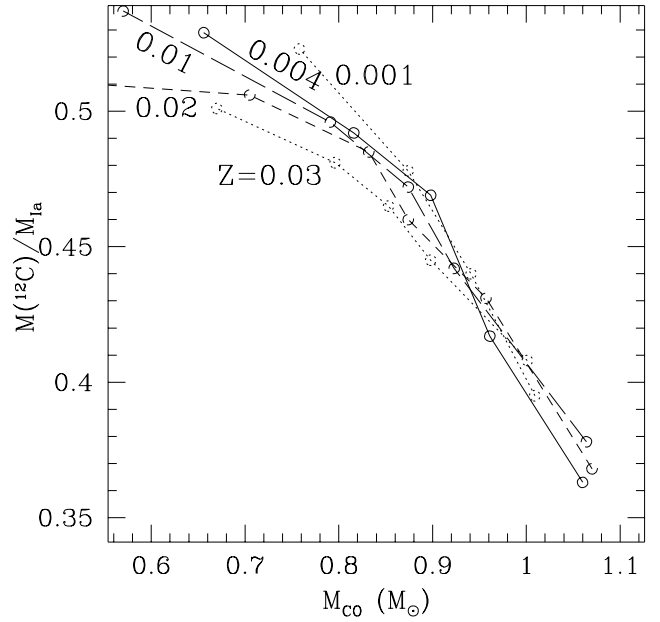


FIG. 12.— Total  $^{12}\text{C}$  mass ( $M(^{12}\text{C})$ ) included in the WD of mass  $M_{\text{Ia}} = 1.37M_{\odot}$  just before an SN Ia explosion as a function of  $M_{\text{CO}}$ . (right)